Double Blind Holography of Attosecond Pulses

O. Pedatzur[*1], A. Trabattoni[2,3], B. Leshem[1], H. Shalmoni[1], M. C. Castrovilli[4,5], M. Galli[2,4], M. Lucchini[2,4], E. Månsson[4], F. Frassetto[6], L. Poletto[6], B. Nadler[7], O. Raz[1], M. Nisoli[2,4], F. Calegari[3,4,8], D. Oron[1] and N. Dudovich[†1]

[1]Department of Physics of Complex Systems, Weizmann Institute of Science, 76100, Rehovot, Israel
[2]Department of Physics, Politecnico di Milano, Piazza Leonardo da Vinci 32, 20133, Milano, Italy
[3]Center for Free-Electron Laser Science, DESY, Notkestr. 85, 22607, Hamburg, Germany
[4]Institute for Photonics and Nanotechnologies, CNR-IFN, Piazza Leonardo da Vinci 32, 20133, Milano, Italy
[5]Inst. for the Structure of Matter CNR-ISM, Area Ricerca di Roma 1, Monterotondo, Italy
[6]Institute for Photonics and Nanotechnologies CNR-IFN, Via Trasea 7, 35131, Padova, Italy
[7]Department of Computer Science and Applied Mathematics, Weizmann Institute of Science, 76100, Rehovot, Israel
[8]Department of Physics, Hamburg Universität, Hamburg, Germany

A key challenge in attosecond science is the temporal characterization of attosecond pulses. Current characterization methods, based on nonlinear light-matter interactions, are limited in terms of stability and waveform complexity. Here we experimentally demonstrate a conceptually new linear and all-optical pulse characterization method, inspired by double blind holography. Holography is realized by measuring the XUV spectra of two unknown attosecond signals and of their interference. Assuming a finite pulse duration constraint, we reconstruct the missing spectral phases and characterize the unknown signals in both isolated pulse and double pulse scenarios. This method can be implemented in a wide range of experimental realizations, enabling the study of complex electron dynamics via a single-shot and linear measurement.

Isolated attosecond pulses are unique tools for studying the natural time scale of electronic processes within matter. A fundamental building block in attosecond time-resolved spectroscopy is the ability to precisely characterize their temporal shape. These pulses encode valuable structural and dynamical information, combining attosecond timing accuracy with Ångstrom spatial precision. This informa-

---

[*]e-mail: orenpedatzur@gmail.com
[†]e-mail: nirit.dudovich@weizmann.ac.il

tion is of key importance for understanding the evolution of electronic wavefunctions in atoms [1], molecules [2, 3, 4, 5, 6] and solids [7]. Studying such phenomena requires the development of a complete and robust characterization method for attosecond pulses, posing one of the primary challenges in this field.

Clearly, the short duration of attosecond pulses, well below the temporal resolution of detector electronics, does not allow for direct characterization in the time domain. Therefore, their measurement is performed in the spectral domain, leading to the loss of spectral phase information. One approach to recover the lost spectral information is to measure the interference of different frequency components. However, as such an interference cannot be obtained via linear measurements, it requires nonlinear light-matter interaction. Commonly used methods, FROG-CRAB (frequency resolved optical gating for complete reconstruction of attosecond bursts) [8, 9] and RABBITT (Reconstruction of attosecond beating by interference of two-photon transitions) [1, 10] involve a nonlinear interaction of the attosecond pulse with the near infrared (NIR) fundamental field. Interferometric autocorrelation can be achieved via the use of an XUV-XUV nonlinear interaction [11, 12]. Finally, the measurement can rely on the intrinsic nonlinearity of the production process itself [13, 14]. Yet, all these time-resolved nonlinear measurements require repetitive measurements at various delays between multiple fields, and are sensitive to noise. Due to the limitations of available techniques, some state-of-the-art attosecond sources, such as X-ray FEL, are difficult to adequately characterize.

In this work we experimentally demonstrate a conceptually different approach to directly measure and characterize XUV attosecond pulses. In contrast with commonly used femtosecond and attosecond characterization methods, our method is based on a *linear measurement* of the XUV spectrum, obviating the need to mix different XUV frequencies. This approach, termed double blind holography (DBH), relies on two key components. The first component is perhaps the most fundamental property of attosecond pulses – a finite temporal duration, also known as a "compact support" (CS) in the time domain. The second component is a spectral measurement of XUV signals from two independent coherent sources as well as their interference, defining a double blind temporal hologram. Figure 1(a) depicts how such "temporal hologram" can be obtained, where each arm of the interferometer represents an independent attosecond source, while the spectral measurement acts as a beam combiner which resolves their interference. Temporal holograms can be realized in a range of experimental systems – from polarization measurements [15] to two sources [16] and even multi-orbital contributions [3]. In our work we implement this scheme using attosecond pulses generated in a mixture of two gases. We further demonstrate the ability to perform a single-shot realization of DBH via the interference between two time delayed pulses.

2

Linear phase retrieval schemes have been extensively used in the spatial domain for the retrieval of objects from their diffraction pattern, as in x-ray lensless imaging or electron diffraction, where the retrieved object is two-dimensional. Indeed, for 2D objects having a finite support, a densely sampled diffraction pattern is sufficient for the reconstruction of phase information [17, 18, 19, 20, 21]. In contrast, the problem of reconstructing an ultrashort temporal 1D signal from its measured spectrum is ill posed, having multiple valid solutions [22, 23]. Holography, another common phase measurement scheme, relies on an a known reference signal. In holography, interference with a known signal maps the missing phase into intensity modulation of the measured signal. Yet, the generation of a well-characterized reference for attosecond temporal holography is extremely difficult. Double blind holography is a scheme which combines a compact support constraint together with holography using an unknown reference, so as to overcome both their individual limitations. This concept has been applied in the spatial domain to retrieve the diffraction phase in coherent diffractive (lensless) imaging scenarios in the visible [24] and X-ray regimes [25]. Here, we apply this scheme in the temporal domain and demonstrate its ability to perform a linear reconstruction of isolated attosecond pulses.

In the following, we briefly describe the essence of the method. For a detailed theoretical study of this method, its advantages and limitations, see [26, 27]. Consider two discretized XUV spectra, each of length N. Their spectral phases define a set of $2N$ unknowns, $X_n^A = e^{i\phi_n^A}$ and $X_n^B = e^{i\phi_n^B}$ with $n = 0, 1, \ldots, N-1$. A compact support (CS) constraint in the time domain requires that the Fourier transform of the pulse spectrum vanishes outside of the support. This constraint introduces a set of $2(N-T)$ linearly independent equations (eqs. (3)-(4) in the Methods section), where T is the width of the CS. Measuring the spectral interference of the two pulses allows for direct reconstruction of their spectral phase difference, $\phi_n^B - \phi_n^A$, forming an additional set of N linear equations (eqs. (1)-(2) in the Methods section). Overall these three measurements provide us with an excess of linear equations which removes the degeneracy associated with the 1D classical phase retrieval problem, allowing its direct reconstruction [26]. Importantly, this method does not require a-priori knowledge of the correct CS. Instead, we scan over potential CS widths and apply the DBH algorithm for each assumed CS. In each iteration we calculate an error score (see Method Section, eq. (7)), which quantifies the residual energy outside of the assumed CS. The estimated CS is the global minimum of this error score. Realistically, the spectral measurements are accompanied by additive noise. Furthermore, the temporal signals may have decaying tails that leak out of the CS. Investigation of the quality of reconstruction in the presence of noise and for exponentially decaying signals can be found in [27].
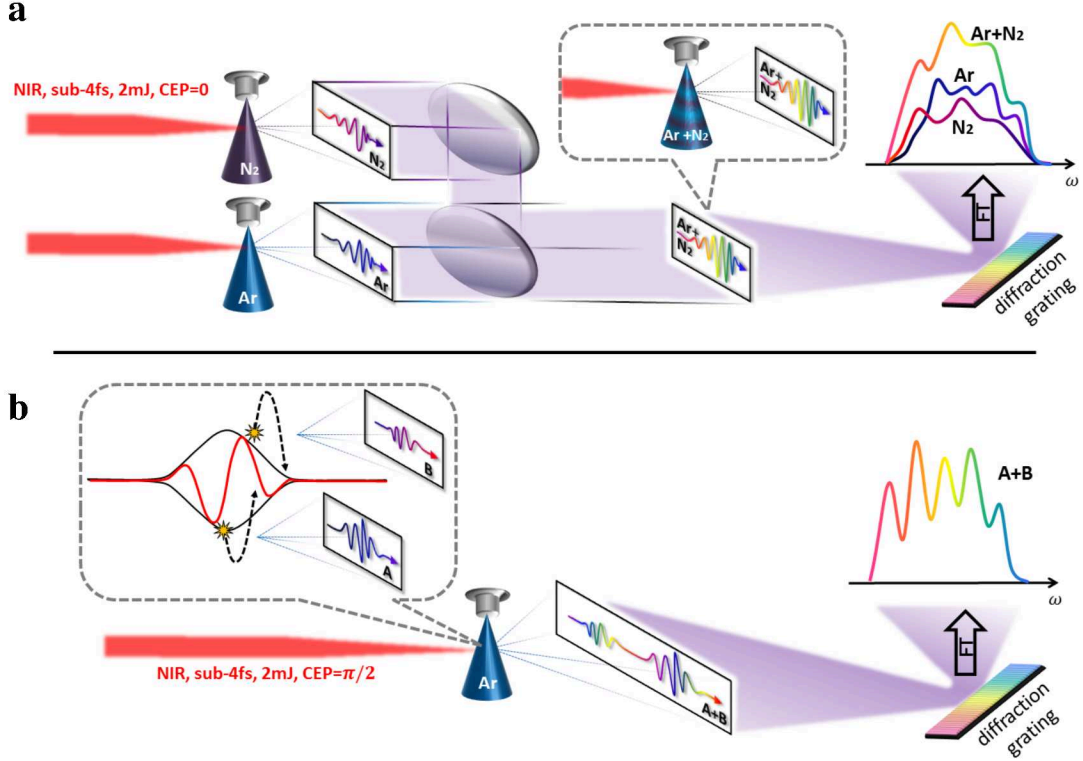
Figure 1: **A schematic description of temporal double blind holography.** (a) Gas mixture DBH: the two arms of the hologram represent the HHG spectrum, produced from Ar and N_2, respectively. The spectral interference between the two arms is achieved by producing HHG in Ar and N_2 gas mixture. (b) Single-shot DBH: in $CEP \sim \pi/2$ configuration, two consecutive half-cycles of the driving field produce two different attosecond pulses delayed by half a period of the NIR. The interference between these two pulses gives rise to spectral fringes.

We experimentally realized DBH of attosecond pulses using the following system. A sub-4 fs, 1-mJ, 800-nm, carrier-envelope phase (CEP) stabilized pulse was focused into a gas cell. The pressure in the cell was regulated by a leak valve under varying backing pressures: 3 bars N_2 and 1 bar Argon (Ar) separately, and their mixture. The generated XUV and the NIR beams pass through a 100-nm-thick aluminum filter which filters out all wavelengths corresponding to energies below 15 eV ($\omega \sim 2.3 \times 10^{16}$ rad/s). The XUV spectrum is measured by an XUV spectrometer, with a spectral threshold accepting energies above 20 eV ($\omega \sim 3 \times 10^{16}$ rad/s). Figure 2(a) shows the three XUV spectra associated with the two attosecond pulses and their interference. The structural difference between the ground state of Ar and N_2 leads to the generation of two significantly different attosecond XUV pulses. The similar ionization potentials of the two gases, $I_p^{Ar} = 15.8$ eV, $I_p^{N_2} = 15.6$ eV, give rise to a broad spectral overlap region over which the relative phase can be extracted. Using low gas density ensures that propagation effects are negligible and that the mixture spectrum indeed represents a coherent addition of the pure gas cases.

Given the three measured spectra and the extracted phase difference, we next apply the DBH algorithm for CS values in the range $0 - 1.35$ fs. We identify a global minimum in the error score curve at $T \sim 640$ as, corresponding to the estimated CS (fig. 2(b)). Figures 2(c-d) present the retrieved spectral phases (solid orange) obtained by DBH at the estimated CS, along with the original spectra for both Ar and N_2 (solid blue). The spectral phases exhibit pronounced group delay dispersion, $GDD_{Ar} = 8 \times 10^{-33} s^2$ and $GDD_{N_2} = 7 \times 10^{-33} s^2$, and also some higher order terms. The gray area represents the uncertainty of the reconstruction procedure. We estimate this area by choosing CS values shifted from the minimum by ± 80 as (one temporal resolution step). Naturally, the uncertainty grows at regions of low signal. We note that any spectral phase-only filter applied to both of the pulses will not affect the measured spectra. Such ambiguity cannot be resolved by the DBH approach [26].

We validate our reconstructions by comparing the retrieved pulses with a FROG-CRAB characterization. Maintaining the same experimental conditions, we focus the unknown XUV pulses together with a NIR beam into a second Neon target where we perform the FROG-CRAB measurement. Here, the strong NIR field serves as a temporal gate for XUV photo-ionized electrons, mapping their pulse properties into their electron momenta. Experimentally, we scan the delay between the NIR and XUV fields and measure the photoelectron spectrum using an electron time-of-flight (TOF) detector (for details see supplementary). Figures 2(c-d) compare the photo-electron spectrum in both gases as measured by the TOF spectrometer (dashed blue) and shifted by I_p. The XUV and photo-electron spectra do not
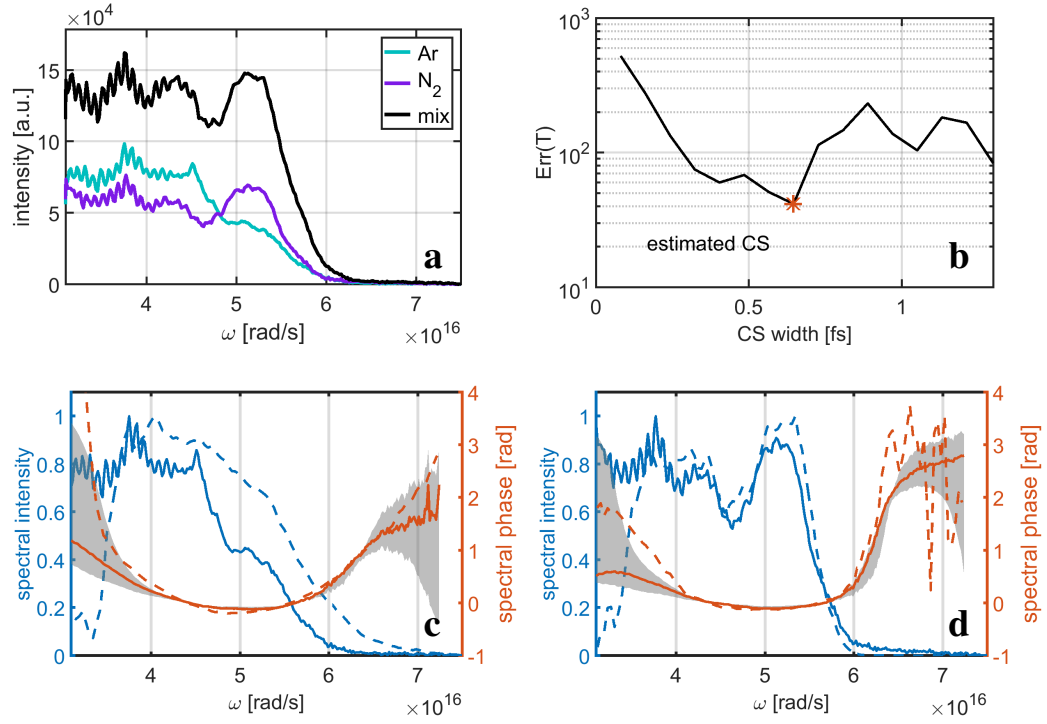
Figure 2: **Gas mixture single pulse DBH.** (a) XUV spectra from three different gases: Ar, N_2 and their mixture. Frequencies below 3×10^{16} rad/s are not detected in our spectrometer. (b) The error score curve and the estimated CS, found at global minimum of the curve. The normalized XUV spectral intensity (solid blue) together with the DBH retrieved spectral phase (solid orange) at the evaluated CS for Ar (c) and N_2 (d). The gray area marks the possible uncertainty in the spectral phase due to inaccurate choice of the CS. The normalized photo-electron spectrum (dashed blue) and the FROG-CRAB retrieved phase (dashed orange) are plotted for comparison.

match perfectly mainly due to the TOF response function. Both the Neon ionization dipole and the fact that low energy electrons are not effectively collected cause a deviation at low energies (frequencies). At low electron kinetic energies standard FROG-CRAB algorithms fail to accurately reconstruct the attosecond pulse. To overcome this problem we combined quick and noise-robust ePIE reconstruction [28] with VTGPA [29] (see supplementary for details). The FROG-CRAB spectral phase reconstruction (dashed orange), obtained after 2000 iteration of the ePIE code and refined by 100 iterations of the VTGPA code, is in close agreement with the DBH result. Deviations appear only at very high frequencies where both signals are relatively weak and at low frequencies where the TOF spectrometer count is low. The FROG-CRAB measurement averages multiple attosecond pulse realizations, that unfortunately are not all identical and differ due to intensity and CEP fluctuations of the NIR field. In contrast, the linear nature of DBH allows for a faster characterization and enables post-selection of spectra obtained under similar experimental conditions (see supplementary for more information).

Double blind holography of attosecond pulses is not limited to the gas mixture realization. Next, we take an important step forward, demonstrating the ability to perform DBH using a *single-shot* measurement. Single-shot DBH has been first demonstrated in the spatial domain [25]. The diffraction of two (or more) finite objects which are separated by more than twice their size allows the extraction of their individual spectra and relative spectral phase directly from the auto-correlation (AC) signal. In this case the two well separated objects serve as unknown references to one another, representing the two arms of the hologram, fig. 1(b). In this paper we demonstrate the temporal analog of this scheme by considering two finite pulses which are delayed by more than twice their individual CS size.

Single-shot DBH is demonstrated by tuning the CEP of the driving pulse in order to generate two attosecond pulses, separated by half the optical period of the fundamental field. Figure 3(a) shows the intensity spectrum measured in Ar gas, showing deep spectral modulations. The modulation period corresponds to a delay between the two pulses of 1.35 fs, exceeding the expected CS of each individual pulse, thus satisfying the basic requirement for single shot reconstruction. Figure 3(b) describes the AC signal, with a main peak and strong side bands arising from the single-object autocorrelations and cross-correlations, respectively. By applying a Fourier transform on the separate peaks we are able to retrieve the individual spectra of the two interfering pulses and their relative phase (see Supplementary).

As in the single pulse case, we search for the optimal CS width and identify a clear minimum at $T = 490$ as, fig. 3(c). The retrieved spectral amplitudes and spectral phase, associated with each attosecond pulse, are presented in fig. 3(e-f). The difference in pulse intensities is attributed to envelope and saturation effects. The expected spectral phase chirp appears clearly in both pulses, where

the gray sleeves indicate a spectral phase error arising from ± 70 as choices of the CS. The stronger pulse has GDD comparable to the single pulse case, $GDD_A = 6 \times 10^{-33} s^2$, whereas for the weaker pulse we find a higher value, $GDD_B = 1.1 \times 10^{-32} s^2$. This effect is dominated by the NIR pulse envelope and can be explained in the electron trajectory picture. Electron trajectories launched at the first half-cycle are driven by a strong returning force whereas trajectories launched at the second half cycle are influenced by a weaker returning force, and exhibit higher dispersion in arrival times. We have approximated this effect using a classical trajectory simulation at our experimental conditions and found that the expected GDDs are $8 \times 10^{-33} s^2$ for the stronger pulse, and $1.3 \times 10^{-32} s^2$ for the weaker pulse, in good agreement with the reconstructed values. Better accuracy can be achieved by taking into account the effects of tunneling and compression in the Al filter.

In conclusion, we have introduced a conceptually new approach to address a key challenge in ultrafast measurements – phase retrieval for ultra-short temporal signals – demonstrating a direct and linear reconstruction of attosecond pulses. Double blind holography can be realized in a wide range of experimental schemes, from polarization measurement to transient gratings or multiple orbitals HHG. In order to demonstrate the versatility of DBH, we have applied this method in two different scenarios: gas mixture and spectral interference of delayed pulses. In contrast to current time-domain nonlinear approaches, our approach is essentially a single-shot measurement. This removes the primary limitations in the characterization of a range of novel ultrafast sources as X-ray FEL attosecond pulses or attosecond plasma mirrors. Looking forward, temporal double blind holography can be implemented to characterize such sources and allow instant attosecond pulse diagnostics. Using this new tool to study complex electron dynamics may give rise to a new class of time-resolved experiments, where attosecond-scale phenomena can be observed using a linear, single-shot measurement.

Methods Let $A_n = |A_n|e^{i\phi_n^A} = \sum_{t=0}^{N-1} a_t e^{2\pi itn/N}$ and $B_n = |B_n|e^{i\phi_n^B} = \sum_{t=0}^{N-1} b_t e^{2\pi itn/N}$ be the discrete Fourier transforms (dft) associated with the two ultrashort signals $\{a_t, b_t\}_{t=0}^{N-1}$ respectively. In a DBH, the spectral intensity of the two signals, $|A_n|^2, |B_n|^2$, and the spectral intensity of their coherent sum, $|A_n + B_n|^2 = |\sum_{t=0}^{N-1}(a_t + b_t)e^{2\pi itn/N}|^2$, are measured. The goal is to characterize the temporal signals $\{a_t, b_t\}_{t=0}^{N-1}$, or equivalently, recover the missing spectral phase vectors $X_n^A = e^{i\phi_n^A}$ and $X_n^B = e^{i\phi_n^B}$, both of length N.

The relative spectral phases $\phi_n^B - \phi_n^A$ are extracted from the intensity measure-
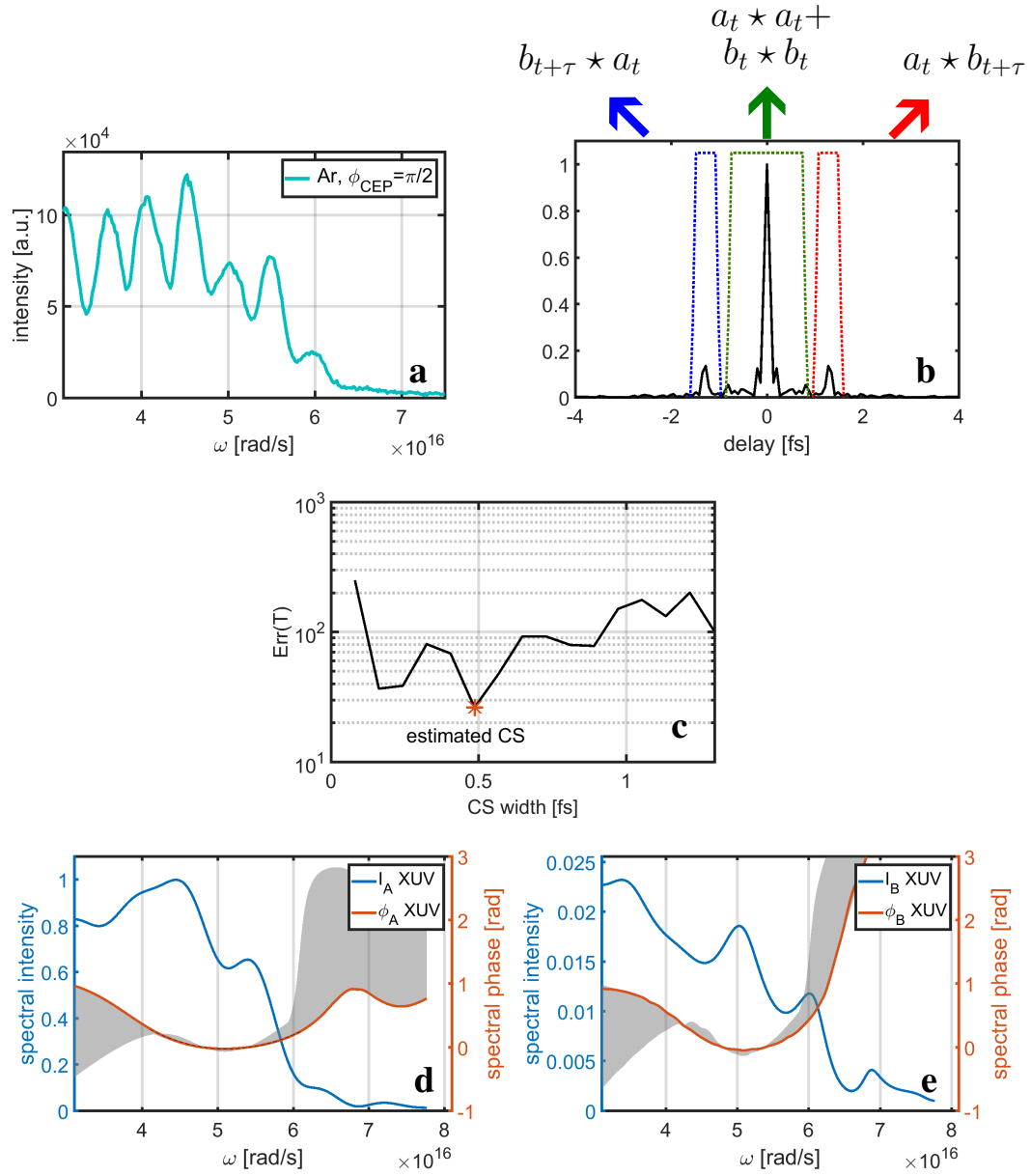
Figure 3: **Single shot double pulse DBH.** By setting the CEP phase to $\sim \pi/2$ we generate two consecutive attosecond pulses in Ar. The two pulses interfere in the spectral domain producing spectral fringes (a). The autocorrelation signal (absolute value) shows the main lobe and two side-peaks, separated by 1.35 fs (half period of the driving field) (b). The main lobe corresponds to the sum of single-pulse autocorrelations, and the side-peaks correspond to cross-correlations. We "cut-out" the different peaks according to the dashed windows and extract the individual pulse spectra and spectral phase difference. (c) The error score curve and the estimated CS, found at global minimum of the curve. Phase retrieval results: (d-e) The normalized XUV spectral intensity (solid blue) together with the DBH retrieved spectral phase (solid orange) at the evaluated CS for the two individual pulses. The gray area marks the possible uncertainty in the spectral phase due to inaccurate choice of the CS.

9

ments according to:

$$\phi_n^B - \phi_n^A = \arccos\left(\frac{|A_n + B_n|^2 - |A_n|^2 - |B_n|^2}{2|A_n B_n|}\right) \tag{1}$$

In general, there exists a sign ambiguity associated with the inverse cosine branches [30]. However, in our specific setting such a zero crossing does not occur. Eq. (1) can be formulated as a set of N linear equations for the unknown phase vectors X_n^A, X_n^B as follows:

$$|A_n||B_n|X_n^A = A_n B_n^* X_n^B \tag{2}$$

The CS constraint of width T constitutes a second set of $2N - 2T$ linear equations for the unknown phase vectors, X_n^A, X_n^B, as follows:

$$\frac{1}{N}\sum_{n=0}^{N-1}|A_n|X_n^A e^{2\pi itn/N} = 0 \quad \text{for} \quad t \notin CS \tag{3}$$

$$\frac{1}{N}\sum_{n=0}^{N-1}|B_n|X_n^B e^{2\pi itn/N} = 0 \quad \text{for} \quad t \notin CS \tag{4}$$

We solve these linear equations for each CS value in a range of feasible CS sizes, returning the suggested solutions $\hat{X}_n^A, \hat{X}_n^B$. These solutions correspond to the following temporal signals,

$$\hat{a}_t = \frac{1}{N}\sum_{n=0}^{N-1}|A_n|\frac{\hat{X}_n^A}{|\hat{X}_n^A|}e^{2\pi itn/N} \tag{5}$$

$$\hat{b}_t = \frac{1}{N}\sum_{n=0}^{N-1}|B_n|\frac{\hat{X}_n^B}{|\hat{X}_n^B|}e^{2\pi itn/N} \tag{6}$$

For each CS guess we calculate an error score. This score expresses the normalized amount of energy leaking out of a suggested CS:

$$Err(T) = \frac{\sum_{t>T}|\hat{a}_t|^2}{\sum_t|\hat{a}_t|^2} + \frac{\sum_{t>T}|\hat{b}_t|^2}{\sum_t|\hat{b}_t|^2} \tag{7}$$

The estimated CS and the output solution of DBH are those corresponding to the global minimum in this error score.

The above procedure is slightly modified for the two delayed pulses. The inverse Fourier transform of the spectral interference of two pulses delayed by τ is

$$IFT[|A_n + e^{2\pi i\tau n/N}B_n|^2] = a_t \star a_t + b_t \star b_t + a_t \star b_{t+\tau} + b_{t+\tau} \star a_t \tag{8}$$

where $\star$ is the cross-correlation operator. When a_t, b_t are temporally separated, the different terms in the AC can be used to deduce $|A_n|^2 + |B_n|^2$, $e^{-2\pi i\tau n/N} A_n B_n^*$ and $e^{2\pi i\tau n/N} A_n^* B_n$. The problem of recovering $|A_n|, |B_n|$ and $A_n B_n^*$ is equivalent to the sign ambiguity mentioned above.

References

[1] Paul, P. M. *et al.* Observation of a train of attosecond pulses from high harmonic generation. *Science* **292**, 1689–1692 (2001).

[2] Sansone, G. *et al.* Electron Localization Following Attosecond Molecular Photoionization. *Nature* **465**, 763–766 (2010).

[3] Smirnova, O. *et al.* High harmonic interferometry of multi-electron dynamics in molecules. *Nature* **460**, 972–977 (2009).

[4] Diveki, Z. *et al.* Spectrally resolved multi-channel contributions to the harmonic emission in N2. *New J. Phys.* **14**, 023062 (2012).

[5] Calegari, F. *et al.* Ultrafast electron dynamics in phenylalanine initiated by attosecond pulses. *Science* **346**, 336–339 (2014).

[6] Nisoli, M., Decleva, P., Calegari, F., Palacios, A. & Martn, F. Attosecond electron dynamics in molecules. *Chem. Rev.* **117**, 10760–10825 (2017). PMID: 28488433.

[7] Garg, M. *et al.* Multi-petahertz electronic metrology. *Nature* **538**, 359–363 (2016).

[8] Mairesse, Y. & Quéré, F. Frequency-resolved optical gating for complete reconstruction of attosecond bursts. *Phys. Rev. A* **71**, 011401 (2005).

[9] Sansone, G. *et al.* Isolated single-cycle attosecond pulses. *Science* **314**, 443–446 (2006).

[10] Mairesse, Y. *et al.* Attosecond synchronization of high-harmonic soft x-rays. *Science* **302**, 1540–1543 (2003).

[11] Tzallas, P., Charalambidis, D., Papadogiannis, N., Witte, K. & Tsakiris, G. D. Direct observation of attosecond light bunching. *Nature* **426**, 267–271 (2003).

[12] Nabekawa, Y. *et al.* Interferometric autocorrelation of an attosecond pulse train in the single-cycle regime. *Phys. Rev. Lett.* **97**, 153904 (2006).

[13] Kim, K. T. *et al.* Manipulation of quantum paths for space-time characterization of attosecond pulses. *Nat. Phys.* **9**, 159–163 (2013).

[14] Mairesse, Y. *et al.* High harmonic xuv spectral phase interferometry for direct electric-field reconstruction. *Phys. Rev. Lett.* **94**, 173903 (2005).

[15] Levesque, J. *et al.* Polarization state of high-order harmonic emission from aligned molecules. *Phys. Rev. Lett.* **99**, 243001 (2007).

[16] Camper, A. *et al.* High-harmonic phase spectroscopy using a binary diffractive optical element. *Phys. Rev. A* **89**, 043843 (2014).

[17] Bruck, Y. M. & Sodin, L. On the ambiguity of the image reconstruction problem. *Opt. Commun.* **30**, 304–308 (1979).

[18] Barakat, R. & Newsam, G. Necessary conditions for a unique solution to two-dimensional phase recovery. *J. Math. Phys.* **25**, 3190–3193 (1984).

[19] Klibanov, M. V., Sacks, P. E. & Tikhonravov, A. V. The phase retrieval problem. *Inverse Probl.* **11**, 1 (1995).

[20] Miao, J., Sayre, D. & Chapman, H. Phase retrieval from the magnitude of the fourier transforms of nonperiodic objects. *J. Opt. Soc. Am. A* **15**, 1662–1669 (1998).

[21] Miao, J., Ishikawa, T., Anderson, E. H. & Hodgson, K. O. Phase retrieval of diffraction patterns from noncrystalline samples using the oversampling method. *Phys. Rev. B* **67**, 174104 (2003).

[22] Hayes, M., Lim, J. & Oppenheim, A. Signal reconstruction from phase or magnitude. *IEEE Transactions on Acoustics, Speech, and Signal Processing* **28**, 672–680 (1980).

[23] Beinert, R. & Plonka, G. Ambiguities in one-dimensional discrete phase retrieval from fourier magnitudes. *J. Fourier Anal. Appl.* **21**, 1169–1198 (2015).

[24] Raz, O. *et al.* Direct phase retrieval in double blind fourier holography. *Opt. Express* **22**, 24935–24950 (2014).

[25] Leshem, B. *et al.* Direct single-shot phase retrieval from the diffraction pattern of separated objects. *Nat. Commun.* **7** (2016).

[26] Raz, O. *et al.* Vectorial phase retrieval for linear characterization of attosecond pulses. *Phys. Rev. Lett.* **107**, 133902 (2011).

[27] Raz, O., Dudovich, N. & Nadler, B. Vectorial phase retrieval of 1-d signals. *IEEE Trans. Signal Processing* **61**, 1632–1643 (2013).

[28] Lucchini, M. *et al.* Ptychographic reconstruction of attosecond pulses. *Opt. Express* **23**, 29502–29513 (2015).

[29] Keathley, P. D., Bhardwaj, S., Moses, J., Laurent, G. & Krtner, F. X. Volkov transform generalized projection algorithm for attosecond pulse characterization. *New J. Phys.* **18**, 073009 (2016).

[30] Leshem, B., Raz, O., Jaffe, A. & Nadler, B. The discrete sign problem: uniqueness, recovery algorithms and phase retrieval applications. *Appl. Comput. Harmon. Anal.* (2017).